

Article

Biofilm-Induced Corrosion Inhibition of Q235 Carbon Steel by *Tenacibaculum mesophilum* D-6 and *Bacillus* sp. Y-6

Xiaoxi Ruan ^{1,2,†}, Linlin Yang ^{1,2,†}, Yan Wang ^{1,2}, Yizhe Dong ^{1,2}, Dake Xu ^{1,2,*} and Mingxing Zhang ^{1,2,*}¹ Shenyang National Laboratory for Materials Science, Northeastern University, Shenyang 110819, China² Electrobiomaterials Institute, Key Laboratory for Anisotropy and Texture of Materials (Ministry of Education), Northeastern University, Shenyang 110819, China

* Correspondence: xudake@mail.neu.edu.cn (D.X.); zhangmingxing@mail.neu.edu.cn (M.Z.)

† Those authors contributed equally to this work.

Abstract: The corrosion of carbon steel causes dramatic economic losses each year. Since conventional corrosion prevention approaches may cause pollution problems to the environment, ecofriendly and effective corrosion approaches are desired. Microbiologically influenced corrosion inhibition (MICI) has been reported as a sustainable corrosion prevention method. This work aims to evaluate the corrosion inhibition effect of two bacterial strains, *Tenacibaculum mesophilum* D-6 and *Bacillus* sp. Y-6 by choosing Q235 carbon steel as a model system. Scanning electron microscopy (SEM), confocal laser scanning microscopy (CLSM) and a series of electrochemical techniques were applied to study the corrosion prevention effect. The electrochemical and pitting results indicated that *T. mesophilum* D-6 displayed a better corrosion protection effect. *T. mesophilum* D-6 formed a denser and thicker biofilm on the Q235 surface than *Bacillus* sp. Y-6. The maximum thickness of the *T. mesophilum* D-6 biofilms was $11.6 \pm 0.7 \mu\text{m}$, which is about twice as thick than that of *Bacillus* sp. Y-6. The corrosion prevention mechanism was ascribed to the formation of biofilms as a barrier to block corrosive agents such as O_2 . This study provides a theoretical foundation for the application of biofilms as green and effective corrosion inhibitors for carbon steel.

Keywords: Q235 carbon steel; *Tenacibaculum mesophilum* D-6; *Bacillus* sp. Y-6; corrosion inhibition; biofilm formation ability



Citation: Ruan, X.; Yang, L.; Wang, Y.; Dong, Y.; Xu, D.; Zhang, M. Biofilm-Induced Corrosion Inhibition of Q235 Carbon Steel by *Tenacibaculum mesophilum* D-6 and *Bacillus* sp. Y-6. *Metals* **2023**, *13*, 649. <https://doi.org/10.3390/met13040649>

Academic Editors: Mosab Kaseem and Yadir Torres Hernández

Received: 19 February 2023

Revised: 20 March 2023

Accepted: 23 March 2023

Published: 25 March 2023



Copyright: © 2023 by the authors. Licensee MDPI, Basel, Switzerland. This article is an open access article distributed under the terms and conditions of the Creative Commons Attribution (CC BY) license (<https://creativecommons.org/licenses/by/4.0/>).

1. Introduction

Steel is widely used in many fields as a structural material. The advantages of Q235 steel include low cost and high ductility and weldability. The major problem of Q235 is its vulnerability to corrosion, which can cause dramatic economic losses and serious safety issues [1,2]. To prevent corrosion, numerous types of methods have been created, such as physical, chemical and electrochemical ideas. Physical corrosion prevention approaches are accomplished by making a physical barrier between the metal surface and the environment, which is also termed coating. Coatings, as one of the easiest and cheapest methods to prevent corrosion, can be generally classified into four types [3]: metallic coatings, conversion coatings, inorganic coatings and paints [4–7]. The application of coatings is limited by two facts. First, coatings must be properly and well made, otherwise they can quickly fail and result in even worse corrosion. Second, coatings may contain toxic organic compounds, which are harmful to the environment [8]. Indeed, hazards to the environment and to ecology induced by the application of conventional corrosion prevention and protection methods have been widely reported [4,5,9]. For the sustainable development of society, long-lasting and ecofriendly corrosion prevention and protection technologies are still appealing.

Microorganisms were mostly considered as the reason for metal corrosion in the past. Microbiologically influenced corrosion (MIC) has been extensively investigated [10,11]. Several MIC mechanisms have been raised, such as extracellular electron transfer (EET) [12–14],

metabolite corrosion [15–19] and the concentration differential battery [20–23]. In recent years, microbiologically influenced corrosion inhibition (MICI) has increasingly attracted attention. MICI was first reported in 1987 by Iverson, who found the inhibition of copper corrosion by bacteria [24]. Recently, Lou summarized MICI mechanisms as follows: the removal of corrosive substances by respiration of microorganisms; the formation of an extracellular polymeric substances (EPSs) layer to protect metals; a microbiologically produced mineralized layer; competitive microbial corrosion inhibition; and corrosion inhibitors secreted by bacteria [25].

Aerobic microorganisms can consume dissolved oxygen through aerobic respiration. Then, a low-oxygen or oxygen-free region forms on the metal surface due to the consumption of oxygen by microorganisms. Since oxygen is a major reason for corrosion, limited oxygen in the environment caused by aerobic respiration of microorganisms prevents metals from corrosion by blocking the cathode reaction [25]. Pedersen explored the inhibition of steel corrosion by two marine bacterial strains, *Pseudomonas* sp. S9 and *Serratia marcescens* EF190 [26], demonstrating that the corrosion inhibition effect was the result of the metabolic activity of bacteria, including oxygen consumption [26]. Chongdar found that the aerobic bacteria *Pseudomonas cichorii* inhibited the corrosion of mild steel by forming biofilms on the metal surface [27].

Bacterial cells in biofilms are embedded in EPSs, which contain complex components such as polysaccharides, proteins, lipids and nucleic acids [28]. EPSs are the fundamental component of biofilms, which stabilize the biofilm structure. Hydrophobic components in EPSs, such as fatty acids, can prevent corrosion by forming an inhibition barrier [25]. In addition to forming an inhibition barrier, EPSs also reduce the adhesion of microorganisms to metal surfaces. Stadler found that the purified EPSs isolated from *Desulfovibrio vulgaris* biofilms inhibited the stay of microorganisms on a highly alloyed steel surface [29]. In 2015, Moradi discovered the corrosion inhibition effect of marine *Vibrio neocaledonicus* sp. to carbon steel [30]. They found that the homogenous biofilm formed on carbon steel inhibited the diffusion of corrosive-agent oxygen ions on the metal surfaces [30]. Liu reported the inhibition effect of EPSs extracted from an iron-oxidizing bacterium on the corrosion of Q235 carbon steel [31].

Microbiologically induced mineralization plays a critical role in chemical cycling and deposition in the nature [25]. Mineralized layers by microorganisms include the phosphate mineralized layer, iron oxide mineralized layer and carbonate mineralized layer [25]. In addition to protecting metals against corrosion, mineralized layers also have the functionality to repair damaged coatings. For example, Volkland found that microbe-induced phosphorylation by *Pseudomonas putida* can repair damaged vivianite coatings on carbon steel surfaces [32].

Many MICI studies have been reported; however, the application of microorganisms to inhibit corrosion on a large scale are still limited. The effect of microorganisms on metal corrosion largely depends on the environmental condition. For instance, electroactive microorganisms, such as the *Shewanella* species, can inhibit corrosion in aerobic conditions by consuming oxygen near the metal surface, but enhance corrosion in anaerobic conditions through the extracellular electron transfer pathway. The effect of temperature on MICI is still not clarified yet, though many studies on the influence of temperature on corrosion inhibition efficiency of abiotic approaches have been reported [33–36]. The heterogeneity of biofilms on metal surfaces also makes it hard to obtain a constant corrosion inhibition performance. Indeed, the selection of suitable microorganisms for application under different conditions is a critical and not yet thoroughly resolved problem [33–36]. To apply microorganisms as green and effective inhibitors, the corrosion inhibition mechanism of bacteria still requires thorough investigation.

In this work, Q235 carbon steel and two bacterial strains, *Tenacibaculum mesophilum* D-6 and *Bacillus* sp. Y-6, were selected as the model system to explore the corrosion inhibition mechanism by microorganisms. The MICI performances of these two bacteria were systematically studied with a variety of electrochemical methods and surface analytical

techniques. Biofilms formed on Q235 carbon steel were observed with confocal laser scanning microscopy (CLSM). The corrosion morphology of carbon steel was characterized by scanning electron microscopy (SEM) and CLSM. The systematic study on the MICI mechanisms of these two bacterial strains can provide a theoretical foundation for their application as green and effective corrosion inhibitors.

2. Materials and Methods

2.1. Bacterial and Materials

T. mesophilum D-6 and *Bacillus* sp. Y-6 was obtained from Prof. Danqing Feng's group (Ocean and Earth College, Xiamen University). The bacterial strains were stored in $-80\text{ }^{\circ}\text{C}$ freezer. The following steps were used to reculture the bacteria. After cultivating on 2216E medium for 24 h at $30\text{ }^{\circ}\text{C}$, 1 mL of bacterial suspension was centrifuged at 8000 rpm for 3 min and washed with PBS twice. The bacterial pellet was resuspended in PBS medium until the OD600 values reached 0.5. The Q235 carbon steel used in this study was obtained from the Institute of Metal Research, Chinese Academy of Sciences (Shenyang, China).

The 2216E medium was ordered from Qingdao Hope Biotechnology Co., Qingdao, China. Phosphate-buffered saline (PBS) was ordered from Aladdin Biochemical Technology Co., Ltd., Shanghai, China. The LIVE/DEAD BacLight Bacterial Viability kit was ordered from Thermo Fisher Scientific Co., Ltd., Eugene, OR, USA.

2.2. Electrochemical Measurements

All electrochemical experiments were carried out using a three-electrode system connected with an electrochemical station (Reference 600, Gamry Instruments, Warminster, PA, USA). A saturated calomel electrode (SCE) was used as the reference electrode. A platinum electrode was used as the auxiliary electrode. The Q235 carbon steel coupons were the working electrodes. The specimens were cut into blocks with dimensions of $1.0 \times 1.0 \times 0.2\text{ cm}$. The exposed surface was polished with silicon carbide metallurgical papers from 240 to 1000 grit. All samples were ultrasonically rinsed in absolute alcohol for 15 min and sterilized with ultraviolet light for 30 min before the immersion tests. All coupons were cold-mounted in epoxy, with copper lines spot-welded onto the back for electrical contact. Then, the exposed surface was polished again with 1000-grit carbide metallurgical papers to obtain an even surface.

Linear polarization resistance (LPR), electrochemical impedance spectroscopy (EIS) and potentiodynamic polarization curve were measured after the open circuit potential (OCP) was stable. LPR was measured with a scanning rate of 0.125 mV/s ranging from -5 mV to $+5\text{ mV}$ vs. E_{OCP} . EIS data were collected with a frequency range between 0.01 and $1 \times 10^5\text{ Hz}$ and an amplitude of $\pm 10\text{ mV}$. To analyze EIS data, ZsimpWin software (Version 3.30, Princeton Applied Research, Oak Ridge, TN, USA) was used. The polarization curves were scanned from -300 mV and $+300\text{ mV}$ versus OCP with a scan rate of 0.333 mV/s . To determine the Tafel slopes, corrosion potential (E_{corr}) and corrosion current density (i_{corr}), the linear parts of cathodic polarization curves were used for Tafel extrapolation. Linear region of cathodic polarization curves was selected from $E_{\text{corr}} - 120\text{ mV}$ to E_{corr} for fitting. The fitting was accomplished by using Gamry Echem Analyst and OriginPro software. All electrochemical experiments were performed in a glass electrolytic cell containing 200 mL of 2216E medium. The media were autoclaved before use. A water bath was used to keep the temperature at $30\text{ }^{\circ}\text{C}$ for the glass electrolytic cell. All experiments were repeated at least three times.

2.3. Surface Analysis and Biofilm Characterization

Biofilm characterization: Scanning electron microscopy (SEM, EVO 10, ZEISS, Oberkochen, Germany) was applied to characterize the biofilm morphology on different samples. After incubation for 7 days, Q235 coupons were washed twice in PBS (1 mL) and then fixed by 5% glutaraldehyde at $4\text{ }^{\circ}\text{C}$ for 2 h. The fixed samples were gradually de-

hydrated with 20, 40, 60, 80 and 100% ethanol for 15 min. In order to facilitate SEM imaging, the surface conductivity of tested samples was first improved by sputtering with Au.

Living biofilms formed on coupons were investigated by a bacterial live/dead staining assay (Invitrogen, Thermo Fisher Scientific, Carlsbad, CA, USA). Briefly, after different treatments, the biofilm cells were costained by Propidium Iodide (PI) and SYTO-9 dyes for 25 min in the dark, followed by washing twice with PBS. According to the instructions from the manufacturer, all live bacteria would be labeled by SYTO-9 and showed green fluorescence, while dead bacteria would be stained by PI and revealed red fluorescence. Finally, fluorescence images were captured using confocal laser scanning microscopy (CLSM, LSM 900, ZEISS, Oberkochen, Germany). The SYTO-9 and PI dyes were excited with 488 and 560 nm laser, respectively. The 3D biofilm morphometry was imaged by z-scan with CLSM.

The 3D profiles of corrosion pits formed on surfaces were imaged with the CLSM. Similarly, ultrasound was used to remove the biofilms and corrosion products before imaging. The maximum pit depth and averaged maximum pit depth were calculated from measured deep/wide pits. The distribution of depth/width of pits was statistically estimated with the confidence interval of 80% [37]. Five maximum pitting depths measured in different regions on the coupon were averaged to calculate averaged maximum pitting depth.

2.4. Weight Loss and Corrosion Product Analysis

After incubation in 2216E medium (with or without bacteria) for 7 days at 30 °C, the biofilm and corrosion products on the sample surfaces were first detached. Briefly, metals were put into ultrasound for 30 min and then rinsed with hydrochloric acid (50%) for 5 s. The sample surfaces were then gently wiped to clean corrosion products. Each sample was then sonicated in absolute ethanol for 30 min and then dried in air. The weight of each sample was measured with an analytical balance with the precision of 0.0001 g (Mettler-Toledo, ME204, Columbus, OH, USA).

After incubation in different culture for 7 days, the corrosion products on Q235 carbon steel surfaces were analyzed with SEM in combination with energy-dispersive spectroscopy (EDS). A small region was selected on each sample. Then, EDS was used to semiquantitatively analyze the composition of corrosion products within the area. The relative contents of each composition, such as Fe, O, C, Na, Cl, were also calculated.

3. Results

3.1. Biofilm Characterization

Biofilm formation on the metal surface is essential to the corrosion behavior of the material. The morphology of *T. mesophilum* D-6 and *Bacillus* sp. Y-6 biofilms on the surface of Q235 carbon steel samples was characterized with scanning electron microscopy (SEM) and confocal laser scanning microscopy (CLSM) after 7 d incubation. As shown in Figure 1a,c, after 7 d incubation, both bacterial strains grew on the metal surface. Compared with *Bacillus* sp. Y-6, *T. mesophilum* D-6 formed relatively denser biofilms. *T. mesophilum* D-6 cells aggregated and formed large clusters, but *Bacillus* sp. Y-6 cells were sparsely distributed on the surface. Besides the biofilm, small dots were also observed, which might be corrosion products. The 3D-CLSM images of biofilms after live/dead staining are shown in Figure 1b,d. The green and red fluorescences represent the live and dead cells, respectively. The yellow color usually represents the overlap of the live and dead cells. As shown in Figure 1b,d, the red and yellow colors were hardly observed. This meant that there were very few dead cells in *Bacillus* sp. Y-6 and *T. mesophilum* D-6 biofilms. The green color also indicated that both *T. mesophilum* D-6 and *Bacillus* sp. Y-6 biofilms grew well on the Q235 coupon surface. The average thickness of the *T. mesophilum* D-6 biofilms was $11.6 \pm 0.7 \mu\text{m}$, which is larger than that of *Bacillus* sp. Y-6 biofilms ($6.2 \pm 1.9 \mu\text{m}$). Dense and thick biofilms may provide a better corrosion protection effect by functioning as a physical barrier against corrosion agents, such as O_2 , Cl^- and acidic reagents.

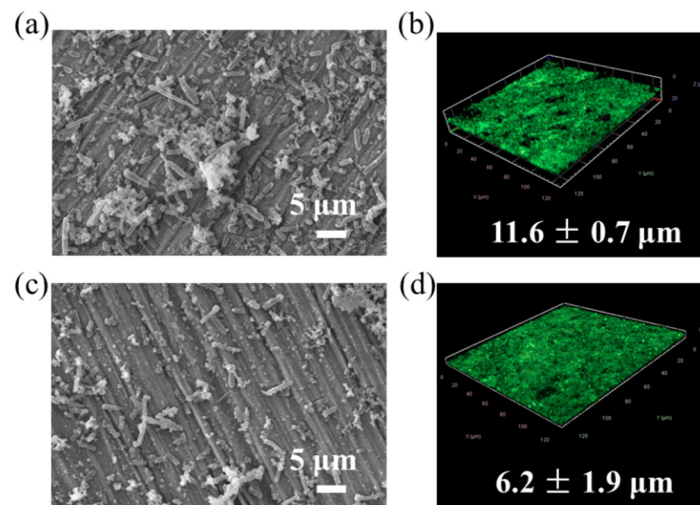


Figure 1. SEM and CLSM images of biofilms grown on Q235 coupons after seven days immersion in different culture media: (a,b) *T. mesophilum* D-6, (c,d) *Bacillus* sp. Y-6. Green color represents live cells with high metabolic activity.

3.2. Electrochemical Tests

Various electrochemical methods were applied to characterize the corrosion prevention and protection effects of *T. mesophilum* D-6 and *Bacillus* sp. Y-6. The E_{OCP} for the Q235 coupons submerged in different conditions are shown in Figure 2a. The E_{OCP} values of the Q235 coupons immersed in the sterilized media fluctuated around 620 mV during 7 days of immersion. With respect to the sterilized condition, the E_{OCP} values of the coupons submerged in cell culture were relatively more stable during 7 days of immersion. The negatively shifted E_{OCP} under biotic conditions may reflect the thermodynamic tendency of the metal sample to occur corrosion reactions. However, the kinetics of the corrosion reaction need to be evaluated by other electrochemical parameters, such as the polarization resistance R_p .

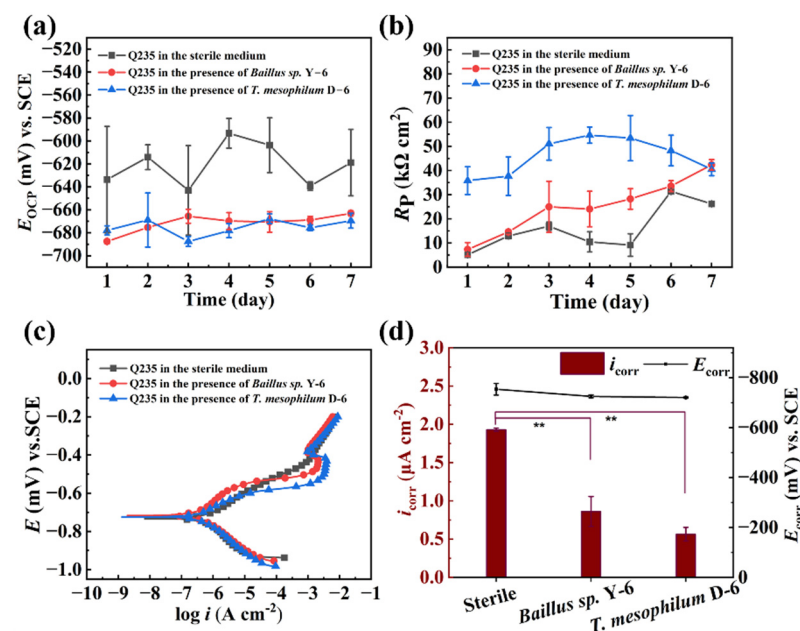


Figure 2. Electrochemical measurements of Q235 coupons in different culture media: (a) E_{OCP} , (b) R_p , (c) potentiodynamic polarization curves after 7 days incubation and (d) corresponding corrosion current density and corrosion potential. The black, red and blue curves represent results of sterile media, *T. mesophilum* D-6 and *Bacillus* sp. Y-6 cultures.

The R_p values were obtained with the LPR test and are shown in Figure 2b. In the abiotic system, the R_p values gradually rose from $5.1 \pm 1.0 \text{ k}\Omega \text{ cm}^2$ to about $26.17 \pm 0.2 \text{ k}\Omega \text{ cm}^2$ during the 7-day experiment. According to the Stern–Geary equation, the increased R_p value usually indicated a decreased corrosion rate [38]. The increased R_p value in the sterile media was due to the gathering of corrosion products on the coupon surfaces. The R_p values of the Q235 coupons submerged in the *Bacillus* sp. Y-6 culture were slightly higher than the abiotic system, indicating its corrosion inhibition effect. The R_p values of the Q235 coupons submerged in the *T. mesophilum* D-6 culture were much higher than those in the *Bacillus* sp. Y-6 culture and the abiotic media, indicating the better corrosion inhibition effect of *T. mesophilum* D-6. The R_p results of the tested Q235 coupons were in the following order: *T. mesophilum* D-6 > *Bacillus* sp. Y-6 > abiotic media. Since *T. mesophilum* D-6 formed denser and thicker biofilms on Q235 coupon surfaces than *Bacillus* sp. Y-6, the corrosion protection effect could be attributed to the biofilm formation abilities of these two bacterial strains.

The potentiodynamic polarization curves of the Q235 samples after 7 days of immersion in sterile media and bacterial cultures were shown in Figure 2c. With respect to the sterile media, the existence of *T. mesophilum* D-6 and *Bacillus* sp. Y-6 decreased both the cathodic reaction and anodic reaction rate. Indeed, the higher cathodic Tafel slopes were observed for Q235 carbon steel in the presence of *Bacillus* sp. Y-6 and *T. mesophilum* D-6, compared with that in the sterile 2216E culture, indicating the decrease in the anodic dissolution rate. Figure 2d showed the corresponding fitted electrochemical parameters. The corrosion current density (i_{corr}) and corrosion potential (E_{corr}) were obtained by fitting the curve (Figure 2d). With respect to the sterile media, the addition of bacteria resulted in a decrease in i_{corr} . The smaller i_{corr} indicated the decreased corrosion rate. The i_{corr} decreases induced by the *T. mesophilum* D-6 and *Bacillus* sp. Y-6 strains were comparable.

The EIS data were analyzed using the equivalent circuits shown in Figure S1. The corresponding fitted parameters are listed in Table S1. After 7 days of immersion, Q_1 and Q_2 of the biotic systems were much smaller than that of the sterile medium. The lowered Q_1 and Q_2 may reflect the increase in the electrical double layer thickness, which was induced by the formation of biofilms and corrosion products on the metal surfaces [39,40]. The decreased Q_1 and Q_2 also indicated the protective effect of the films that were composed with biofilms and corrosion products.

After inoculating bacterial cells for one day, the R_{ct} of the sterile media, *Bacillus* sp. Y-6 and *T. mesophilum* D-6 were 3911, 4650 and 26,110 $\Omega \cdot \text{cm}^2$, respectively. The largest R_{ct} value of indicated its highest corrosion inhibition effect. After immersion for 4 days, the R_{ct} of the sterile media, *Bacillus* sp. Y-6 and *T. mesophilum* D-6 increased to 6974, 20,830 and 42,290 $\Omega \cdot \text{cm}^2$, respectively. The increase in R_{ct} of the sterile system was due to the accumulation of corrosion products on the metal surface, while the increased R_{ct} of the biotic systems were due to the formation of biofilms and corrosion products. The increased R_{ct} of the sample in the *Bacillus* sp. Y-6 and *T. mesophilum* D-6 culture also demonstrated the increasing corrosion inhibition effect with the growing of biofilms on Q235 coupon surfaces. After immersion for 7 days, the R_{ct} of the sample in the *Bacillus* sp. Y-6 culture increased to 40,930 $\Omega \cdot \text{cm}^2$, while that in the *T. mesophilum* D-6 culture was 39,510 $\Omega \cdot \text{cm}^2$. The reason for the slight decrease in the R_{ct} in the *T. mesophilum* D-6 on day 7, compared with that on day 4, might be that the *T. mesophilum* D-6 biofilms became mature and achieved their highest corrosion inhibition effect earlier than day 7.

Nyquist and Bode plots for the Q235 samples immersed in the different culture media at 1, 4 and 7 days are presented in Figure 3. As shown in the Nyquist plot (Figure 3a,c,e), the samples in the sterile media always had the smallest diameters of the capacitive semicircles after different immersion times. This indicates that Q235 in the sterile media had the lowest charge-transfer resistance. Thus, the corrosion rate of the sample under sterile media was the highest. This result was in agreement with the i_{corr} data (Figure 2d). Samples immersed in the biotic media were observed to have larger diameters of the capacitive semicircles in Nyquist plots, and the largest diameters appeared with the presence of the *T. mesophilum*

D-6 media. This phenomenon demonstrated that the addition of bacteria inhibited the corrosion of the samples, and the inhibition effect of *T. mesophilum* D-6 was stronger than that of *Bacillus* sp. Y-6. In addition, the diameter of the Nyquist plot in the samples of the biotic media increased with the immersion time, indicating that the corrosion protection effects of the bacterial strains were gradually increasing [41]. Furthermore, the $|Z|$ values in the presence of *T. mesophilum* D-6 at the low-frequency region were the highest, as shown in Bode plots, indicating the highest corrosion resistance of Q235. As shown in Figure 3b,d,f, the $|Z|$ value at the low-frequency region illustrated that the order of the corrosion resistance was *T. mesophilum* D-6 > *Bacillus* sp. Y-6 > abiotic media. This was consistent with the results of the polarization resistance observed in LPR test (Figure 2b). The Bode-phase diagrams showed two time constants for all systems after 7 days of immersion. The one with high frequency may be due to the formation of a protective layer and corrosion products on the metal surface, while the one with low frequencies may be caused by an electrical double layer. For media containing *T. mesophilum* D-6 and *Bacillus* sp. Y-6, the capacitive behavior in the low-frequency region can be attributed to the cumulative capacitive effect due to biofilm formation [42]. Moreover, it can be observed that in media with *T. mesophilum* D-6, the two time constants mentioned above appeared at lowest frequencies, indicating the slowest corrosion reaction rate. The Nyquist and Bode results indicated that *T. mesophilum* D6 had the most significant effect in inhibiting Q235 corrosion.

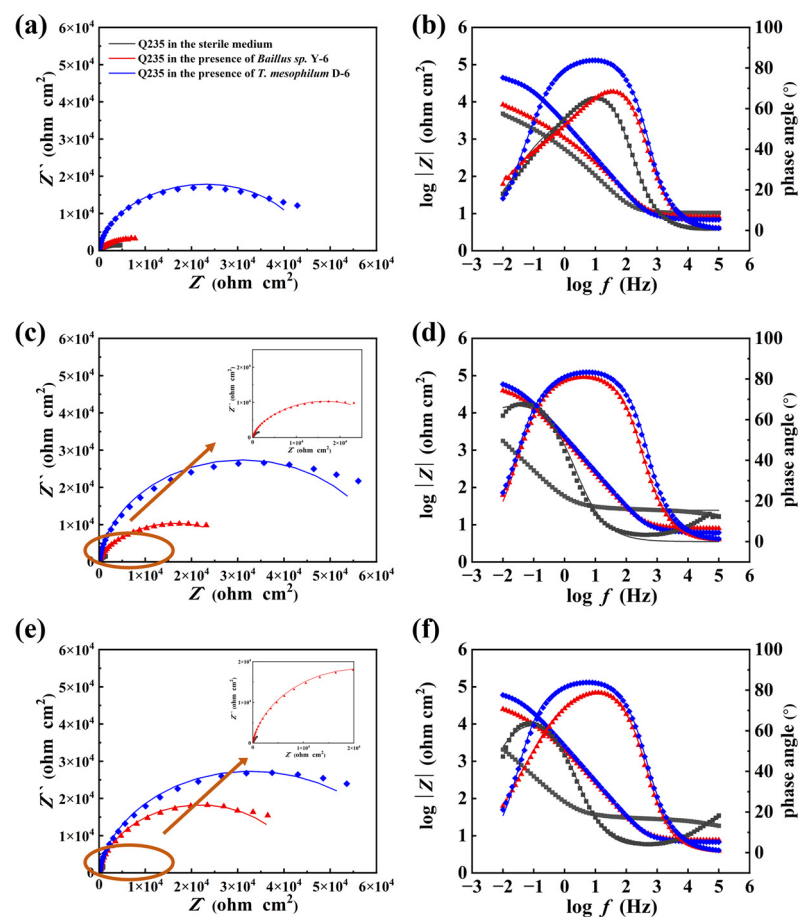


Figure 3. Nyquist (a,c,e) and Bode (b,d,f) plots of Q235 coupons immersed in the different culture media at 1, 4 and 7 days. Insertions in c and e are enlarged pictures of the left bottom corner.

3.3. Weight Loss and Pitting Corrosion

Weight loss tests were carried out to explore the uniform corrosion behavior of Q235 carbon steel under different conditions. The weight loss results are presented in Figure 4a.

After 7 days of immersion, the weight loss of the Q235 carbon steel was $16.1 \pm 3.3 \text{ mg/cm}^2$ in the abiotic medium. Considering the aerobic experimental conditions, the weight loss can be attributed to the result of O_2 corrosion. However, it decreased to 7.3 ± 2.5 and $5.4 \pm 0.9 \text{ mg/cm}^2$ with the addition of *Bacillus* sp. Y-6 and *T. mesophilum* D-6, respectively. The weight loss data reflected that the two test bacterial strains slowed the uniform corrosion of Q235, and *T. mesophilum* D6 displayed the best inhibition effect. To determine if pH played a critical role in the uniform corrosion of Q235, the pHs for each system were detected during the 7-day experiment. As shown in Figure 4b, the pHs of the bacterial culture were around 7.5 during the 7-day experiment. The stable pH value of about 7.5 indicates that the growth of *Bacillus* sp. Y-6 and *T. mesophilum* D-6 did not obviously change the pH. Thus, acid corrosion was not the major contributor to Q235 corrosion.

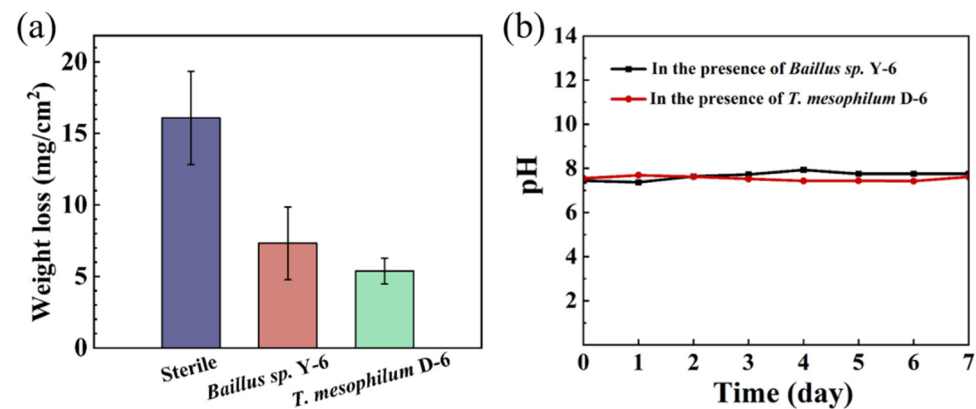


Figure 4. Weight loss of Q235 carbon steel (a) and pH variation (b) in different culture. The black curve and red curve represent the pH change of *Bacillus* sp. Y-6 and *T. mesophilum* D-6, respectively.

The corrosion pits on Q235 sample surfaces were also imaged and analyzed with CLSM. The maximum pitting morphology with the measured depth are shown in Figure 5. After immersion in the sterile media for seven days, the averaged maximum pit depth was $5.7 \pm 0.9 \mu\text{m}$. This phenomenon indicated that corrosive agents (e.g., O_2 , Cl^-) in the media caused localized corrosion on the Q235 surface. For the coupons immersed in the biotic media, much shallower pits were observed. The averaged maximum pit depth decreased to 3.9 ± 0.9 and $2.6 \pm 0.6 \mu\text{m}$ in the presence of *Bacillus* sp. Y-6 and *T. mesophilum* D-6, respectively. The pitting results confirmed the electrochemical results that both bacterial strains inhibited the corrosion of Q235, and *T. mesophilum* D-6 had a stronger inhibitory effect. The corrosion protection effect of two bacterial strains were positively related to the thickness of the biofilm formed on the Q235 surfaces.

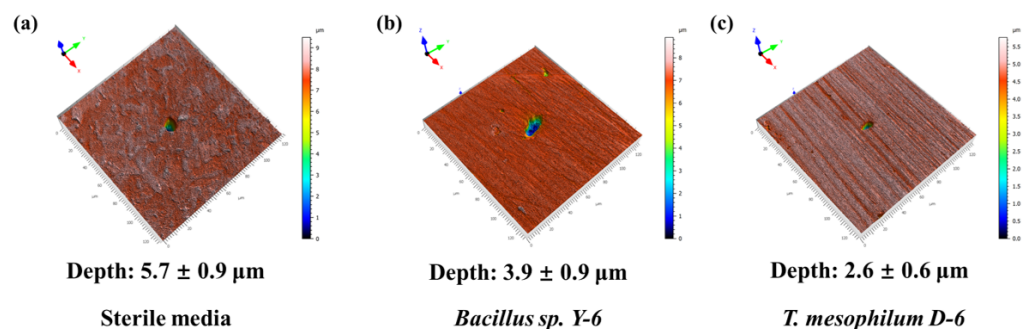


Figure 5. The averaged maximum pitting depth of Q235 coupons at the end of the 7-day incubation in different culture media: (a) sterile media, (b) *Bacillus* sp. Y-6, (c) *T. mesophilum* D-6. Five maximum pitting depths measured in different regions on the coupon were averaged to obtain the averaged value.

The corrosion pits in different groups were also evaluated by statistical analysis with a high confidence level. As shown in Figure 6, the corrosion pit width and depth of Q235 decreased with the presence of *Bacillus* sp. Y-6 and *T. mesophilum* D-6, compared with coupons in the sterile medium. Additionally, *T. mesophilum* D-6 had a better inhibitory performance than *Bacillus* sp. Y-6. The corrosion protection effect of the two bacterial strains had a positive correlation with the thickness of the biofilm on the Q235 surfaces. The pitting results were also consistent with the electrochemical results.

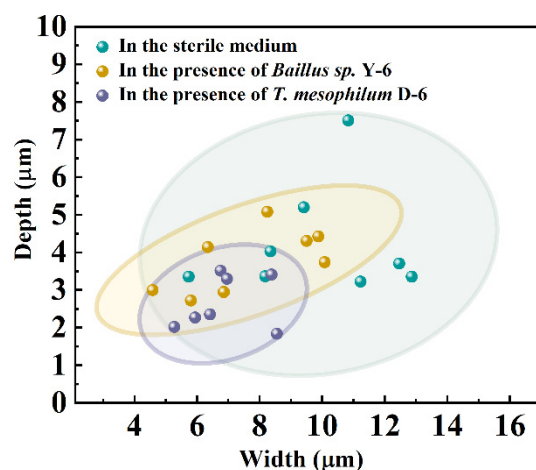


Figure 6. Statistical analysis of pit width/depth after 7 days incubation in different cultures. The green, orange and purple dots represent the result of the sterile medium, *Bacillus* sp. Y-6 and *T. mesophilum* D-6 culture, respectively.

3.4. Corrosion Product Analysis

Analysis of corrosion products can provide insight into the corrosion mechanism from the molecular level. Corrosion product analysis was performed with SEM and EDS. Figure S2 shows the sampling method for EDS. The relative content of Fe, O, C and Na in corrosion products are shown in Table 1. The content of oxygen of the corrosion product in the abiotic condition was $16.7 \pm 7.4\%$. The presence of *Bacillus* sp. Y-6 and *T. mesophilum* D-6 decreased the content of oxygen to $11.7 \pm 3.1\%$ and $6.5 \pm 1.6\%$, respectively. The decreased content of oxygen implied the decreased amount of corrosion product, iron oxides. Thus, the lowered content of oxygen induced by *Bacillus* sp. Y-6 and *T. mesophilum* D-6 indicated their inhibition effect on Q235 corrosion. In agreement with the electrochemical test, weight loss result and pitting analysis, corrosion product analysis also supported that *T. mesophilum* D-6 displayed the best inhibition effect.

Table 1. Content of Fe, O, C and Na in corrosion products obtained with EDS test.

	Fe (Wt %)	O (Wt %)	C (Wt %)	Na (Wt %)
Sterile	44.7 ± 2.4	16.7 ± 7.4	15.2 ± 6.9	12.4 ± 5.5
<i>Bacillus</i> sp. Y-6	67.1 ± 8.5	11.7 ± 3.1	6.4 ± 1.9	7.6 ± 2.1
<i>T. mesophilum</i> D-6	85.9 ± 3.3	6.5 ± 1.6	4.5 ± 1.2	3.2 ± 0.9

4. Discussion

MICI is a potential ecofriendly corrosion inhibition technique. However, systematic studies on the relationship between biofilm formation capability and corrosion protection performance are still in shortage. In this study, two aerobic marine bacteria, *Bacillus* sp. Y-6 and *T. mesophilum* D-6, were utilized to perform corrosion tests on Q235 in simulated seawater. Through surface morphological characterization and corrosion evaluation, both strains were confirmed to have the ability to inhibit corrosion, with *T. mesophilum* D-6 showing a higher inhibitory effect.

The R_p and i_{corr} data showed that both *Bacillus* sp. Y-6 and *T. mesophilum* D-6 slowed the corrosion rate of Q235 in simulated sea water (Figure 2). The EIS results were consistent with the R_p and i_{corr} results. The Nyquist plots of the Q235 sample measured in the *T. mesophilum* D-6 culture displayed the largest diameters, which meant the highest corrosion resistance (Figure 3). The two time constants of the Bode-phase diagrams measured in the *Bacillus* sp. Y-6 and *T. mesophilum* D-6 cultures might be due to the formation of the protective layer and the electrical double layer [42]. The lowest frequencies of the Bode diagram in the *T. mesophilum* D-6 culture demonstrated the slowest corrosion reaction rate. The weight loss and pitting data (Figures 4–6) confirmed the same conclusion.

The surface analysis results of Q235 coupons in the simulated marine environment demonstrated that the ability to form biofilms of the two bacterial strains was different (Figure 1). With respect to *Bacillus* sp. Y-6, *T. mesophilum* D-6 formed denser and thicker biofilms on the Q235 steel and displayed a better corrosion inhibition effect. Thus, we believe that biofilms were the key factors in corrosion inhibition, and the corrosion protection effect was positively correlated with their biofilm formation ability.

The corrosion inhibition effect of biofilms was considered from the following two aspects (Figure 7). First, planktonic and sessile cells consume O_2 to obtain energy through aerobic respiration. Then, low-oxygen or oxygen-free regions were generated on the metal surface. Since dissolved oxygen is a major reason for corrosion in an aqueous environment [43], the metal corrosion was alleviated by the limited cathodic reaction [44]. The decreased content of oxygen (Table 1) due to the presence of *Bacillus* sp. Y-6 and *T. mesophilum* D-6 implied a decrease in oxygen concentration. However, to further confirm this statement, the oxygen concentration in the culture media and within the biofilm are desired to be measured in the future. Second, the EPSs adsorbed on Q235 play a barrier role. EPSs are the main components of the biofilm, which are mainly composed of extracellular polysaccharides, proteins, lipids and nucleic acids [28]. Those polymeric macromolecules can absorb corrosive agents, thus blocking their diffusion to the metal surface. Indeed, isolated and purified EPSs from biofilms have been demonstrated to be the key factor in the corrosion inhibition of biofilms [45,46]. In addition to blocking corrosive agents, EPSs also reduce the adhesion of other microorganisms [29]. In this study, the effects of EPSs in *T. mesophilum* D-6 and *Bacillus* sp. Y-6 biofilms on the corrosion of Q235 carbon steel were proposed. Future work will focus on evaluating the specific functionality of EPSs by isolating EPSs from the biofilm.

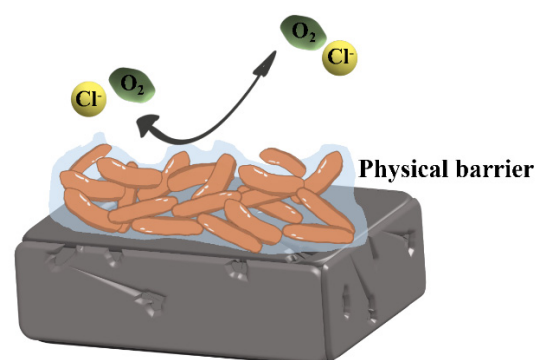


Figure 7. Proposed mechanism of corrosion inhibition of *Bacillus* sp. Y-6 and *T. mesophilum* D-6 biofilms on metal surfaces. The biofilm formed on the metal surface blocks corrosive reagents.

5. Conclusions

In summary, the corrosion inhibition effects of *T. mesophilum* D-6 and *Bacillus* sp. Y-6 on Q235 carbon steel were investigated with SEM, CLSM and electrochemical methods. All acquired data demonstrated that both bacterial strains can inhibit Q235 corrosion. *T. mesophilum* D-6 exhibited better corrosion inhibition performance than *Bacillus* sp. Y-6. SEM and CLSM images showed that *T. mesophilum* D-6 formed denser and thicker biofilms on the Q235 surface than *Bacillus* sp. Y-6. The maximum thickness of *T. mesophilum* D-6 was

$11.6 \pm 0.7 \mu\text{m}$, which was about twice that of the *Bacillus* sp. Y-6 biofilm. The corrosion inhibition effect was ascribed to the biofilm formation capability of the bacterial strain. This study provides a theoretical basis for the use of biofilm as an ecofriendly corrosion inhibitor for carbon steel.

Supplementary Materials: The following supporting information can be downloaded at: <https://www.mdpi.com/article/10.3390/met13040649/s1>, Figure S1: Equivalent circuits used for EIS data analysis. Herein, R_s represents the resistance of the solution, R_{film} is the resistance of the film (biofilm and corrosion products film), R_{ct} is the charge transfer resistance, Q_1 is the capacitance of the film and Q_2 is the capacitance of electrical double layer; Figure S2: The sampling regions for EDS test; Table S1: EIS parameters of Q235 coupons in different culture.

Author Contributions: Conceptualization, D.X., M.Z. and X.R.; data curation, X.R., Y.W. and L.Y.; formal analysis, X.R., L.Y., Y.W. and Y.D.; investigation, X.R., L.Y. and Y.D.; methodology, X.R. and L.Y.; project administration, D.X. and M.Z.; supervision, D.X. and M.Z.; validation, X.R. and M.Z.; visualization, X.R., L.Y., Y.W. and Y.D.; writing—original draft, M.Z. and L.Y.; writing—review and editing, D.X., M.Z., L.Y. and X.R. All authors have read and agreed to the published version of the manuscript.

Funding: This research was funded by the National Natural Science Foundation of China (No. 52101078) and College Student Innovation and Entrepreneurship Training Program (No. 220096) and the Research Fund of State Key Laboratory for Marine Corrosion and Protection of Luoyang Ship Material Research Institute (LSMRI) under the contract No. JS220409.

Data Availability Statement: The data that support the findings of this study are available from the corresponding author upon request.

Conflicts of Interest: The authors declare no conflict of interest.

References

1. Ma, Y.; Li, Y.; Wang, F. Corrosion of low carbon steel in atmospheric environments of different chloride content. *Corros. Sci.* **2009**, *51*, 997–1006. [[CrossRef](#)]
2. Hou, B.; Li, X.; Ma, X.; Du, C.; Zhang, D.; Zheng, M.; Xu, W.; Lu, D.; Ma, F. The cost of corrosion in China. *npj Mater. Degrad.* **2017**, *1*, 4. [[CrossRef](#)]
3. Pedferri, P. Corrosion Prevention by Coatings. In *Corrosion Science and Engineering*; Springer International Publishing: Cham, Switzerland, 2018; pp. 327–361.
4. Hao, X.; Chen, S.; Qin, D.; Zhang, M.; Li, W.; Fan, J.; Wang, C.; Dong, M.; Zhang, J.; Cheng, F.; et al. Antifouling and antibacterial behaviors of capsaicin-based pH responsive smart coatings in marine environments. *Mater. Sci. Eng. C* **2020**, *108*, 110361. [[CrossRef](#)] [[PubMed](#)]
5. Zhang, F.; Ju, P.; Pan, M.; Zhang, D.; Huang, Y.; Li, G.; Li, X. Self-healing mechanisms in smart protective coatings: A review. *Corros. Sci.* **2018**, *144*, 74–88. [[CrossRef](#)]
6. Yang, Z.; Hao, X.; Chen, S.; Ma, Z.; Wang, W.; Wang, C.; Yue, L.; Sun, H.; Shao, Q.; Murugadoss, V.; et al. Long-term antibacterial stable reduced graphene oxide nanocomposites loaded with cuprous oxide nanoparticles. *J. Colloid Interface Sci.* **2019**, *533*, 13–23. [[CrossRef](#)] [[PubMed](#)]
7. Sun, H.; Yang, Z.; Pu, Y.; Dou, W.; Wang, C.; Wang, W.; Hao, X.; Chen, S.; Shao, Q.; Dong, M.; et al. Zinc oxide/vanadium pentoxide heterostructures with enhanced day-night antibacterial activities. *J. Colloid Interface Sci.* **2019**, *547*, 40–49. [[CrossRef](#)] [[PubMed](#)]
8. Furdek, M.; Vahčić, M.; Ščančar, J.; Milačić, R.; Kniewald, G.; Mikac, N. Organotin compounds in seawater and *Mytilus galloprovincialis* mussels along the Croatian Adriatic Coast. *Mar. Pollut. Bull.* **2012**, *64*, 189–199. [[CrossRef](#)]
9. Shen, Y.; Wu, Z.; Tao, J.; Jia, Z.; Chen, H.; Liu, S.; Jiang, J.; Wang, Z. Spraying Preparation of Eco-Friendly Superhydrophobic Coatings with Ultralow Water Adhesion for Effective Anticorrosion and Antipollution. *ACS Appl. Mater. Interfaces* **2020**, *12*, 25484–25493. [[CrossRef](#)]
10. Huang, Y.; Liu, S.J.; Jiang, C.Y. Microbiologically influenced corrosion and mechanisms. *Microbiol. China* **2017**, *44*, 1699–1713.
11. Telegdi, J.; Shaban, A.; Trif, L. 8 - Microbiologically influenced corrosion (MIC). In *Trends in Oil and Gas Corrosion Research and Technologies*; El-Sherik, A.M., Ed.; Woodhead Publishing: Boston, MA, USA, 2017; pp. 191–214.
12. Lovley, D.R. Happy together: Microbial communities that hook up to swap electrons. *Isme J.* **2017**, *11*, 327–336. [[CrossRef](#)]
13. Shi, L.; Dong, H.L.; Reguera, G.; Beyenal, H.; Lu, A.H.; Liu, J.; Yu, H.Q.; Fredrickson, J.K. Extracellular electron transfer mechanisms between microorganisms and minerals. *Nat. Rev. Microbiol.* **2016**, *14*, 651–662. [[CrossRef](#)] [[PubMed](#)]

14. El-Naggar, M.Y.; Wanger, G.; Leung, K.M.; Yuzvinsky, T.D.; Southam, G.; Yang, J.; Lau, W.M.; Neelson, K.H.; Gorby, Y.A. Electrical transport along bacterial nanowires from *Shewanella oneidensis* MR-1. *Proc. Natl. Acad. Sci. USA* **2010**, *107*, 18127–18131. [[CrossRef](#)] [[PubMed](#)]
15. Morales, J.; Esparza, P.; González, S.; Salvarezza, R.; Arévalo, M.P. The role of *Pseudomonas aeruginosa* on the localized corrosion of 304 stainless steel. *Corros. Sci.* **1993**, *34*, 1531–1540. [[CrossRef](#)]
16. Wang, D.; Liu, J.; Jia, R.; Dou, W.; Kumseranee, S.; Punpruk, S.; Li, X.; Gu, T. Distinguishing two different microbiologically influenced corrosion (MIC) mechanisms using an electron mediator and hydrogen evolution detection. *Corros. Sci.* **2020**, *177*, 108993. [[CrossRef](#)]
17. Sowards, J.W.; Mansfield, E. Corrosion of copper and steel alloys in a simulated underground storage-tank sump environment containing acid-producing bacteria. *Corros. Sci.* **2014**, *87*, 460–471. [[CrossRef](#)]
18. Huber, B.; Herzog, B.; Drewes, J.E.; Koch, K.; Müller, E. Characterization of sulfur oxidizing bacteria related to biogenic sulfuric acid corrosion in sludge digesters. *Bmc Microbiol.* **2016**, *16*, 1–11. [[CrossRef](#)]
19. Xu, D.; Li, Y.; Gu, T. Mechanistic modeling of biocorrosion caused by biofilms of sulfate reducing bacteria and acid producing bacteria. *Bioelectrochemistry* **2016**, *110*, 52–58. [[CrossRef](#)]
20. Little, B.J.; Lee, J.S. Microbiologically influenced corrosion: An update. *Int. Mater. Rev.* **2014**, *59*, 384–393. [[CrossRef](#)]
21. Beech, I.B.; Cheung, C.W.S. Interactions of exopolymers produced by sulphate-reducing bacteria with metal ions. *Int. Biodeterior. Biodegrad.* **1995**, *35*, 59–72. [[CrossRef](#)]
22. Javed, M.A.; Neil, W.C.; Stoddart, P.R.; Wade, S.A. Influence of carbon steel grade on the initial attachment of bacteria and microbiologically influenced corrosion. *Biofouling* **2016**, *32*, 109–122. [[CrossRef](#)]
23. Javed, M.A.; Stoddart, P.R.; Wade, S.A. Corrosion of carbon steel by sulphate reducing bacteria: Initial attachment and the role of ferrous ions. *Corros. Sci.* **2015**, *93*, 48–57. [[CrossRef](#)]
24. Iverson, W.P. Microbial Corrosion of Metals. In *Advances in Applied Microbiology*; Laskin, A.I., Ed.; Academic Press: Cambridge, MA, USA, 1987; Volume 32, pp. 1–36.
25. Lou, Y.; Chang, W.; Cui, T.; Wang, J.; Qian, H.; Ma, L.; Hao, X.; Zhang, D. Microbiologically influenced corrosion inhibition mechanisms in corrosion protection: A review. *Bioelectrochemistry* **2021**, *141*, 107883. [[CrossRef](#)] [[PubMed](#)]
26. Pedersen, A.; Hermansson, M. Inhibition of metal corrosion by bacteria. *Biofouling* **1991**, *3*, 1–11. [[CrossRef](#)]
27. Chongdar, S.; Gunasekaran, G.; Kumar, P. Corrosion inhibition of mild steel by aerobic biofilm. *Electrochim. Acta* **2005**, *50*, 4655–4665. [[CrossRef](#)]
28. Li, Z.; Wang, X.; Wang, J.; Yuan, X.; Jiang, X.; Wang, Y.; Zhong, C.; Xu, D.; Gu, T.; Wang, F. Bacterial biofilms as platforms engineered for diverse applications. *Biotechnol. Adv.* **2022**, *57*, 107932. [[CrossRef](#)]
29. Stadler, R.; Wei, L.; Fürbeth, W.; Grooters, M.; Kuklinski, A. Influence of bacterial exopolymers on cell adhesion of *Desulfovibrio vulgaris* on high alloyed steel: Corrosion inhibition by extracellular polymeric substances (EPS). *Mater. Corros.* **2010**, *61*, 1008–1016. [[CrossRef](#)]
30. Moradi, M.; Xiao, T.; Song, Z. Investigation of corrosion inhibitory process of marine *Vibrio neocaledonicus* sp. bacterium for carbon steel. *Corros. Sci.* **2015**, *100*, 186–193. [[CrossRef](#)]
31. Liu, H.W.; Gu, T.Y.; Asif, M.; Zhang, G.A.; Liu, H.F. The corrosion behavior and mechanism of carbon steel induced by extracellular polymeric substances of iron-oxidizing bacteria. *Corros. Sci.* **2017**, *114*, 102–111. [[CrossRef](#)]
32. Volkland, H.P.; Harms, H.; Knopf, K.; Wanner, O.; Zehnder, A.J.B. Corrosion inhibition of mild steel by bacteria. *Biofouling* **2000**, *15*, 287–297. [[CrossRef](#)]
33. Alasvand Zarasvand, K.; Rai, V.R. Microorganisms: Induction and inhibition of corrosion in metals. *Int. Biodeterior. Biodegrad.* **2014**, *87*, 66–74. [[CrossRef](#)]
34. Al-Amiery, A.A.; Mohamad, A.B.; Kadhum, A.A.H.; Shaker, L.M.; Isahak, W.N.R.W.; Takriff, M.S. Experimental and theoretical study on the corrosion inhibition of mild steel by nonanedioic acid derivative in hydrochloric acid solution. *Sci. Rep.* **2022**, *12*, 4705. [[CrossRef](#)] [[PubMed](#)]
35. Videla, H.A.; Herrera, L.K. Understanding microbial inhibition of corrosion. A comprehensive overview. *Int. Biodeterior. Biodegrad.* **2009**, *63*, 896–900. [[CrossRef](#)]
36. Jayaraman, A.; Earthman, J.C.; Wood, T.K. Corrosion inhibition by aerobic biofilms on SAE 1018 steel. *Appl. Microbiol. Biotechnol.* **1997**, *47*, 62–68. [[CrossRef](#)]
37. Michael, F.; Georges, M.; John, F. Elliptical Insights: Understanding Statistical Methods through Elliptical Geometry. *Stat. Sci.* **2013**, *28*, 1–39. [[CrossRef](#)]
38. Zhou, E.; Zhang, M.; Huang, Y.; Li, H.; Wang, J.; Jiang, G.; Jiang, C.; Xu, D.; Wang, Q.; Wang, F. Accelerated biocorrosion of stainless steel in marine water via extracellular electron transfer encoding gene *phzH* of *Pseudomonas aeruginosa*. *Water Res.* **2022**, *220*, 118634. [[CrossRef](#)]
39. Moradi, M.; Song, Z.; Xiao, T. Exopolysaccharide produced by *Vibrio neocaledonicus* sp. as a green corrosion inhibitor: Production and structural characterization. *J. Mater. Sci. Technol.* **2018**, *34*, 2447–2457. [[CrossRef](#)]
40. Popova, A.; Sokolova, E.; Raicheva, S.; Christov, M. AC and DC study of the temperature effect on mild steel corrosion in acid media in the presence of benzimidazole derivatives. *Corros. Sci.* **2003**, *45*, 33–58. [[CrossRef](#)]
41. Lv, M.; Du, M.; Li, X.; Yue, Y.; Chen, X. Mechanism of microbiologically influenced corrosion of X65 steel in seawater containing sulfate-reducing bacteria and iron-oxidizing bacteria. *J. Mater. Res. Technol.* **2019**, *8*, 4066–4078. [[CrossRef](#)]

42. Sheng, X.; Ting, Y.-P.; Pehkonen, S.O. The influence of sulphate-reducing bacteria biofilm on the corrosion of stainless steel AISI 316. *Corros. Sci.* **2007**, *49*, 2159–2176. [[CrossRef](#)]
43. Wang, S.; Yin, X.; Zhang, H.; Liu, D.; Du, N. Coupling Effects of pH and Dissolved Oxygen on the Corrosion Behavior and Mechanism of X80 Steel in Acidic Soil Simulated Solution. *Materials* **2019**, *12*, 3175. [[CrossRef](#)]
44. Kuklinski, A.; Sand, W. Microbiologically Influenced Corrosion. In *Encyclopedia of Applied Electrochemistry*; Kreysa, G., Ota, K.-i., Savinell, R.F., Eds.; Springer: New York, NY, USA, 2014; pp. 1276–1290.
45. Gao, Y.; Zhang, M.; Fan, Y.; Li, Z.; Cristiani, P.; Chen, X.; Xu, D.; Wang, F.; Gu, T. Marine *Vibrio* spp. protect carbon steel against corrosion through secreting extracellular polymeric substances. *npj Mater. Degrad.* **2022**, *6*, 6. [[CrossRef](#)]
46. Li, Z.; Zhou, J.; Yuan, X.; Xu, Y.; Xu, D.; Zhang, D.; Feng, D.; Wang, F. Marine Biofilms with Significant Corrosion Inhibition Performance by Secreting Extracellular Polymeric Substances. *ACS Appl. Mater. Interfaces* **2021**, *13*, 47272–47282. [[CrossRef](#)] [[PubMed](#)]

Disclaimer/Publisher's Note: The statements, opinions and data contained in all publications are solely those of the individual author(s) and contributor(s) and not of MDPI and/or the editor(s). MDPI and/or the editor(s) disclaim responsibility for any injury to people or property resulting from any ideas, methods, instructions or products referred to in the content.